HONOM  2013

EUROPEAN WORKSHOP on High Order Nonlinear Numerical Methods for Evolutionary PDEs, Bordeaux, March 18-22, 2013

A priori-based mesh adaptation for third-order accurate Euler simulation

Alexandre Carabias[†], **Estelle Mbinky**[‡]

([†]) INRIA - Tropics project Sophia-Antipolis, France
([‡])INRIA - Gamma Project Rocquencourt, France
Alexandre.Carabias@inria.fr

Motivation of the study

- Propagation of waves in large spaces.
- Mesh adaptation should follow the wave propagation.
- Adjoint-based adaptation criterion will concentrate on zone of interest for a chosen functional output.
- An accurate approximation scheme needs be chosen.

Scope of the talk

1. Interpolation error analysis
2. Reconstruction error analysis
3. CENO2 Scheme
4. Approximation error analysis
5. Optimal metric
6. Resolution of optimum
7. Numerical experiments
8. Concluding remarks

1. Interpolation error analysis (1)

Π_2: 2D Lagrange quadratic interpolation:

$$|(u - \Pi_2 u)(\delta \mathbf{x})| \approx |P_u(\delta \mathbf{x})|.$$

$\delta \mathbf{x} = (\delta x, \delta y)$ defines mesh size.
The generic error model is a homogeneous polynomial of degree $k = 3$ in 2 variables :

$$P_u(\mathbf{x}) = \sum_{i=0}^{i=3} \binom{k}{i} \; a(u)_i \; x^i \; y^{k-i}$$

$a(u)_i$ are third derivatives of u.

1. Interpolation error error analysis (2): Modeling of the quadratic order interpolation error

Local optimization problem

- Main Idea: $(P_u)^{\frac{2}{3}}$ being homogeneous with a quadratic form with respect to mesh size, let us approach locally the variations of P_u by a quadratic definite positive form taken at power $\frac{3}{2}$, i.e, for $(x, y) \in \mathbb{R}^2$,

$$|P_u(x,y)| \leqslant \left({}^t(x,y)\, \mathcal{S}_u^{loc}\, (x,y) \right)^{\frac{3}{2}}$$

$\Rightarrow$ Find the optimal local metric $\mathcal{S}_u^{loc}$ (optimal local directions and sizes) to construct a majorant of the local error model P_u.

The optimal local metric $\mathcal{S}_u^{loc}$ is the one whose unit ball is the maximum area ellipse included in the isoline 1 of P_u.

1. Interpolation error error analysis (3): Example

⋆ $P_u = 6\,x^3 - 8.594\,x^2 y - 6.98\,xy^2 - 100\,y^3$

- Optimal local metric in P_u
- in $\left({}^t(x,y)\,\mathcal{S}_u^{loc}\,(x,y)\right)^{\frac{3}{2}}$

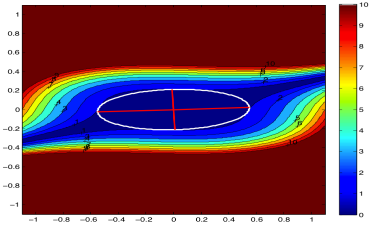

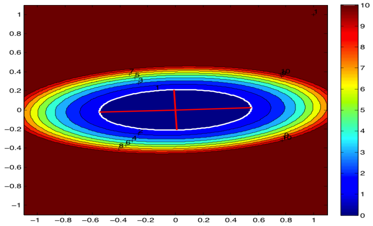

Superposition of the iso-lines of P_u and $\left({}^t(x,y)\,\mathcal{S}_u^{loc}\,(x,y)\right)^{\frac{3}{2}}$

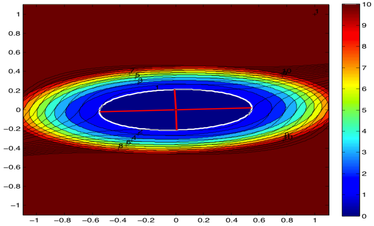

1. Interpolation error error analysis (4)

Construction of optimal local metrics

Binary decomposition by Sylvester's theorem [Brachat-Mourrain, 1999]

$$P_u(x,y) = \sum_{j=1}^{2(rank)} \lambda_j\,(\alpha_j\,x + \beta_j\,y)^{\mathbf{3}} \quad ; \quad \beta_i = 1$$

Real case | Complex case

$$\mathcal{S}_u^{loc} = {}^t\,Q_u \begin{pmatrix} |\lambda_1|^{\frac{2}{3}} & 0 \\ 0 & |\lambda_2|^{\frac{2}{3}} \end{pmatrix} Q_u \qquad \mathcal{S}_u^{loc} = {}^{t_c}Q_u \begin{pmatrix} |\lambda_1|^{\frac{2}{3}} & 0 \\ 0 & |\lambda_2|^{\frac{2}{3}} \end{pmatrix} Q_u$$

$$Q_u = \begin{pmatrix} \alpha_1 & \beta_1 \\ \alpha_2 & \beta_2 \end{pmatrix} ; \; {}^tQ_u = \begin{pmatrix} \alpha_1 & \alpha_2 \\ \beta_1 & \beta_2 \end{pmatrix} \quad ; \quad {}^{t_c}Q_u = \begin{pmatrix} \bar{\alpha}_1 & \bar{\alpha}_2 \\ \bar{\beta}_1 & \bar{\beta}_2 \end{pmatrix}$$

In the complex case, $\lambda_2 = \bar{\lambda}_1$ and $\alpha_2 = \bar{\alpha}_1$.

$\mathcal{S}_u^{loc}$ **is real symmetric in both cases**

Optimal estimate

Find the maximal ellipse inside the $|P_u(\mathbf{x})| = 1$ level set.

$$\Rightarrow \; \widetilde{\mathcal{S}}_u = \; c_{opt} \, \mathcal{S}_u^{loc} \; = \; {}^t\mathcal{R}_u \begin{pmatrix} \tilde{\mu}_1 & 0 \\ 0 & \tilde{\mu}_2 \end{pmatrix} \mathcal{R}_u$$

$$c_{opt} = 1 \;\; \text{real case} \;\; ; \;\; c_{opt} = 2^{-\frac{1}{3}} \;\; \text{complex case.}$$

$$\Rightarrow \;\; |P_u(x,y)| \leqslant \left(\, {}^t(x,y) \, \widetilde{\mathcal{S}}_u \, (x,y) \, \right)^{\frac{3}{2}}$$

Mesh parametrization by a Riemannian metric

For any $\mathbf{x}$ in Ω, $\mathcal{M}(\mathbf{x})$ is a symmetric matrix.

$$\mathcal{M} \;\mapsto\; \mathbf{Mesh}(\mathcal{M})$$

Such that any edge $\mathbf{ab}$ of $Mesh(\mathcal{M})$ has a unit $\mathcal{M}$-length:

$$\int_0^1 \sqrt{{}^t\mathbf{ab}\ \mathcal{M}(\mathbf{a}+t\mathbf{ab})\ \mathbf{ab}}\,\mathrm{d}t = 1.$$

$$\mathcal{M}(\mathbf{x}) = d_{\mathcal{M}}(\mathbf{x})\mathcal{R}(\mathbf{x})\Lambda(\mathbf{x})\mathcal{R}^t(\mathbf{x}) \quad \text{with} \quad det\ \Lambda = 1.$$

• The rotation $\mathcal{R} = (\mathbf{e}_\xi, \mathbf{e}_\eta)$ parametrises the two orthogonal **stretching directions** of the metric.

• Λ is a diagonal matrix with eigenvalues $\lambda_1 = m_\eta/m_\xi$ and $\lambda_2 = m_\xi/m_\eta$ where m_ξ and m_η represent the two directional local mesh sizes in the characteristic/stretching directions of $\mathcal{M}$. λ_1/λ_2 is the **stretching ratio**.

• $d_{\mathcal{M}} = m_\xi^{-1} m_\eta^{-1}$ is the **node density**.

1. Interpolation error error analysis (8)

Find the optimal Riemannian metric $\mathcal{M}$ defined on the computational domain for smallest weighted-L^1 error

$$\min_{\mathcal{M}} \int_\Omega g(\mathbf{x}) \left(trace(\mathcal{M}^{-\frac{1}{2}} |\, \widetilde{\mathcal{S}}_u \,| \mathcal{M}^{-\frac{1}{2}}) \right)^{\frac{3}{2}} d\mathbf{x}$$

$$\text{with} \quad \int_\Omega d(\mathcal{M}) d\mathbf{x} = N$$

$$\Rightarrow \quad \mathcal{M}_{opt} = N \left(\int_\Omega \kappa \; d\mathbf{x} \right)^{-1} \kappa \quad {}^t\mathcal{R}_u \begin{pmatrix} \nu_1 & 0 \\ 0 & \nu_1^{-1} \end{pmatrix} \mathcal{R}_u$$

$$\nu_1 = \left(\frac{\tilde{\mu}_1}{\tilde{\mu}_2} \right)^{-\frac{1}{2}} \quad \kappa = (2g\tilde{\mu}_1\tilde{\mu}_2)^{\frac{3}{5}} \; .$$

2. Reconstruction error error analysis

Vertex, dual cell, 2-exact quadratic reconstruction

Given $\bar{u}_i$ on on each cell i of centroid G_i, find the $c_{i,\alpha}$, $|\alpha| \leq$ **2** s.t.

$$R_2^0 \bar{u}_i(x) = \bar{u}_i + \sum_{|\alpha| \leq 2} c_{i,\alpha}[(X - G_i)^\alpha - \int_{Cell_i} (X - G_i)^\alpha \mathrm{d}\mathbf{x}]$$

$$\overline{R_2^0 \bar{u}} = \int_{Cell_i} R_2^0 \bar{u}_{i,i} \mathrm{d}\mathbf{x} = \overline{u_i} \qquad \sum_{j \in N(i)} (\overline{R_2^0 \bar{u}_{i,j}} - \overline{u_j})^2 = Min \ .$$

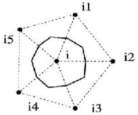

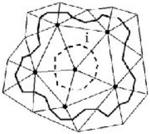

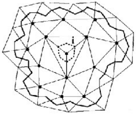

Same treatment as interpolation

R_2: 2D quadratic ENO reconstruction:

$$|u(\mathbf{x}) - R_2^0 u(\mathbf{x})| \approx |\sum_{i=0}^{i=3} \binom{k}{i} a_i x^i y^{k-i}| \leqslant \left(\; {}^t(x,y)\, \widetilde{\mathcal{S}}_u \,(x,y) \; \right)^{\frac{3}{2}}$$

$a(u)_i$ are third derivatives of u.

3. CENO2 Scheme (1)

Variational statement of a model problem

$$B(u,v) = \int_\Omega v \nabla \cdot \mathcal{F}(u)\, \mathrm{d}\Omega - \int_\Gamma v \mathcal{F}_\Gamma(u)\, \mathrm{d}\Gamma,$$

B is linear with respect to v.

Find $u \in \mathcal{V}$ such that $B(u,v) = 0 \ \forall \ v \in \mathcal{V}$.

CENO discrete statement (after C. Groth), vertex version

$$\mathcal{V}_0 = \{v_0, V_0|_{\mathbf{Cell_i}} = const \ \forall \ i \ \textbf{vertex}\}$$

Find $u_0 \in \mathcal{V}_0$ such that $B(R_2^0 u_0, v_0) = 0 \ \forall \ v_0 \in \mathcal{V}_0$

2-exact flux integration

The integral on a cell interface $C_{ij} = C_i \cap C_j$ is split into the integrals on the two segments of C_{ij}.

On each segment $C_{ij}^{(1)}$ and $C_{ij}^{(2)}$ a numerical integration with two Gauss points (two Riemann solvers) is applied.

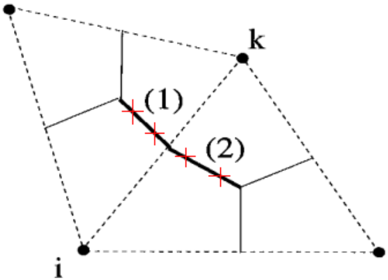

4. *A priori* error analysis (1)

Cf. "*A posteriori* analysis for a large set of p-order reconstruction-based Godunov methods" Barth-Larson 2002.

$$\text{Scalar output} \quad j(u) = (g, u).$$

Projection π_0: $\mathcal{V} \rightarrow \mathcal{V}_0, \ v \mapsto \pi_0 v$

$$\forall \ C_i, \text{dual cell}, \quad \pi_0 v|_{C_i} = \int_{C_i} v dx / meas(C_i).$$

$$\text{Output error} \quad \delta j = (g, R_2^0 \pi_0 u - R_2^0 u_0).$$

The adjoint state $u_0^* \in \mathcal{V}_0$ is the solution of:

$$\frac{\partial B}{\partial u}(R_2^0 u_0)(R_2^0 v_0, u_0^*) = (g, R_2^0 v_0), \ \forall \ v_0 \in \mathcal{V}_0.$$

4. *A priori* error analysis (2)

Simpler case:

$B(u,v)=F(v)$ where B is bilinear, F is linear, for example:
$B(u,v)=\int_\Omega v div(\mathbf{V}u)\mathrm{d}\Omega+\int_\Gamma uv\mathbf{V}\cdot\mathbf{n}\mathrm{d}\Gamma$ and $F(v)=\int_\Gamma u_B v\mathbf{V}\cdot\mathbf{n}\mathrm{d}\Gamma$.

$$\begin{array}{rcll} B(v,u_0^*) & = & (g,v) & \text{(discr.adj. eq.)} \\ B(R_2^0u_0,v) & = & F(v) & \text{(discr.state eq.)} \\ B(u,v) & = & F(v) & \text{(cont.state eq.)} \end{array}$$

$\Rightarrow$

$$\begin{array}{rcll} (g,R_2^0\pi_0u-R_2^0u_0) & = & B(R_2^0\pi_0u-R_2^0u_0,u_0^*) & \text{(discr.adj. eq.)} \\ & \approx & B(R_2^0\pi_0u,u_0^*)-B(R_2^0u_0,u_0^*) & \\ & \approx & B(R_2^0\pi_0u,u_0^*)-F(u_0^*) & \text{(discr.state eq.)} \\ & \approx & B(R_2^0\pi_0u,u_0^*)-B(u,u_0^*) & \text{(cont.state eq.)} \\ & \approx & B(R_2^0\pi_0u-u,u_0^*) & \end{array}$$

The error is directly expressed in terms of the reconstruction error for exact solution.

4. *A priori* error analysis (3)

Unsteady Euler: $W = (\rho, \rho u, \rho v, \rho E)$

For the case of Euler eqs, we get after some calculations:

$$|B(R_2^0\pi_0 W - W, W_0^*)| \approx\leq 2\int_\Omega \sum_q K_q(W, W^*)|R_2^0\pi_0 u_q - u_q|\ \mathrm{d}\Omega$$

with $(u_q)_{q=1,8} = (W, W_t)$,
and in which the $K_q(W, W^*)$ are built from space derivatives of W^* and Euler fluxes derivatives with respect to dependant variable W.

5. Optimal metric (1)

Using the previous reconstruction error estimate:

$$|R_2^0\pi_0 u_q - u_q| \approx \left(trace(\mathcal{M}^{-1/2} S_q \mathcal{M}^{-1/2})\right)^{\frac{3}{2}} \ .$$

Optimization problem

After the *a priori* analysis, we have to minimise the following error:

$$\mathcal{E} \ = \ \int \sum_q K_q(W, W^*) \left(trace(\mathcal{M}^{-1/2} S_q \mathcal{M}^{-1/2})\right)^{\frac{3}{2}} \ dxdy$$

$$= \ \int \left(trace(\mathcal{M}^{-1/2} S \mathcal{M}^{-1/2})\right)^{\frac{3}{2}} \ dxdy$$

$$= \ \int d_{\mathcal{M}}^{-\frac{3}{2}} \left(trace[(\mathcal{R}_{\mathcal{M}} \Lambda_{\mathcal{M}} \mathcal{R}_{\mathcal{M}}^T)^{-\frac{1}{2}} |S| (\mathcal{R}_{\mathcal{M}} \Lambda_{\mathcal{M}} \mathcal{R}_{\mathcal{M}}^T)^{-\frac{1}{2}}]\right)^{\frac{3}{2}} \ dxdy$$

with constraint $\int d_{\mathcal{M}} \ dxdy = N$.

5. Optimal metric (2)

Minimize $\mathcal{E}(\mathcal{M}) =$

$$\int d_{\mathcal{M}}^{-\frac{3}{2}} \left(trace[(\mathcal{R}_{\mathcal{M}}\Lambda_{\mathcal{M}}\mathcal{R}_{\mathcal{M}}^{T})^{-\frac{1}{2}}|S|(\mathcal{R}_{\mathcal{M}}\Lambda_{\mathcal{M}}\mathcal{R}_{\mathcal{M}}^{T})^{-\frac{1}{2}}] \right)^{\frac{3}{2}} \; dxdy$$

with constraint $\int d_{\mathcal{M}} \; dxdy = N.$

Optimal solution:

$\forall \; \mathbf{x} : S = \mathcal{R}_S \bar{\Lambda}_S \mathcal{R}_S^T \;\; \Rightarrow \;\; \mathcal{R}_{\mathcal{M}_{opt}} = \mathcal{R}_S \; , \; \Lambda_{\mathcal{M}_{opt}} = \bar{\Lambda}_S^{-1} / det(S)$

$det(S)^{\frac{3}{2}} (d_{\mathcal{M}_{opt}})^{-\frac{5}{2}} = const.$

$\Rightarrow \;\; d_{\mathcal{M}_{opt}} \;\; = \;\; N \; (\int det(S)^{\frac{3}{5}} \; dxdy)^{-1} det(S)^{\frac{3}{5}}$

$$\mathcal{M}_{opt} = d_{\mathcal{M}_{opt}} \mathcal{R}_{\mathcal{M}_{opt}} \Lambda_{\mathcal{M}_{opt}} \mathcal{R}_{\mathcal{M}_{opt}}^T$$

5. Optimal metric (3): isotropic case

Minimize $\mathcal{E}(\mathcal{M}) =$

$$\int d_{\mathcal{M}}^{-\frac{3}{2}} \left(trace[(\lambda_{\mathcal{M}})^{-\frac{1}{2}}|S|(\lambda_{\mathcal{M}})^{-\frac{1}{2}}] \right)^{\frac{3}{2}} \ dxdy$$

with constraint $\int d_{\mathcal{M}} \ dxdy = N.$

Optimal solution:

$\lambda_{\mathcal{M}_{opt}} = trace[S]^{-1}/det(S)$

$det(S)^{\frac{3}{2}}(d_{\mathcal{M}_{opt}})^{-\frac{5}{2}} = const.$

$\Rightarrow \ d_{\mathcal{M}_{opt}} \ = \ N \ (\int det(S)^{\frac{3}{5}} \ dxdy)^{-1} det(S)^{\frac{3}{5}}$

$$\mathcal{M}_{opt} \ = \ d_{\mathcal{M}_{opt}} \ \lambda_{\mathcal{M}_{opt}}$$

6. Resolution of optimum, unsteady case

The *continuous* model giving the adapted mesh involves a **state system**, an **adjoint system** and the **optimality relation** giving $\mathcal{M}_{opt}$.

We discretise it.

The time discretisation of the metric is made of coarser time intervals.

We solve it.

by the Global Unsteady Fixed Point algorithm of Belme *et al.* JCP2012.

6. Resolution of optimum, unsteady case

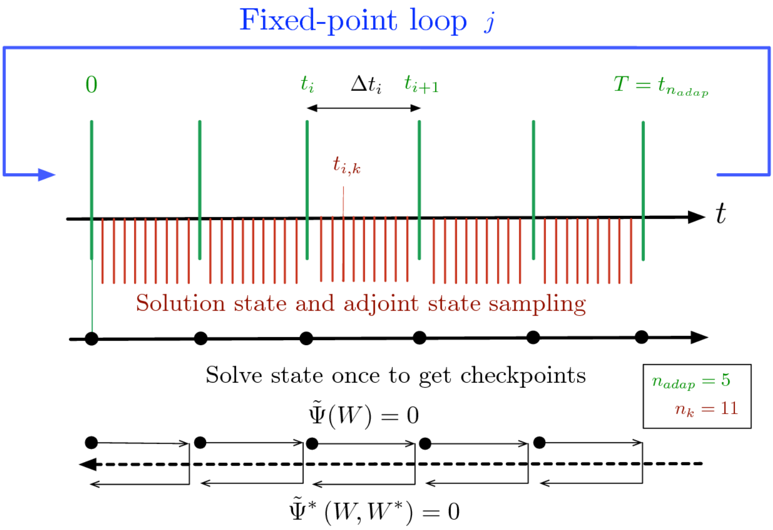

7. Numerical experiments

We present a first series of experiments where the propagation of an acoustical perturbation is followed by the mesh adaptator in order to minimise the mesh effort.

1. Noise wall problem
2. Diffraction problem

7. Numerical experiments: Noise wall problem (1)

Propagation of an acoustic wave from a source while observing the impact on the detector.

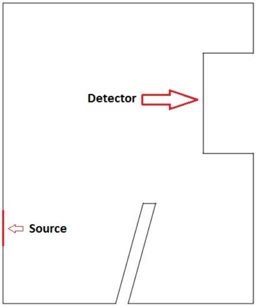

Acoustic source :

$$r = -Ae^{-Bln(2)\left[x^2+y^2\right]}cos(2\pi f).$$

Functional:

$$j(W) = \int_0^T \int_M \frac{1}{2}(p - p_{air})^2 \mathrm{d}M\mathrm{d}t.$$

7. Numerical experiments: Noise wall problem (2)

Density field evolving in time on uniform mesh (line 1), adapted one (middle line), with corresponding adapted meshes (last line):

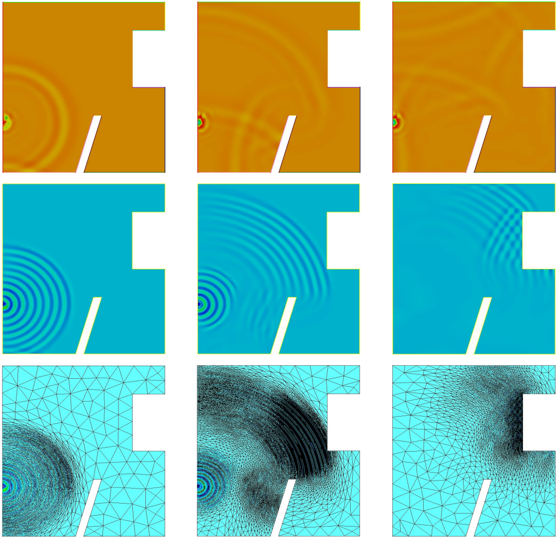

7. Numerical experiments: Noise wall problem (3)

Scalar output comparaison : MUSCL (-) vs CENO (—) schemes.

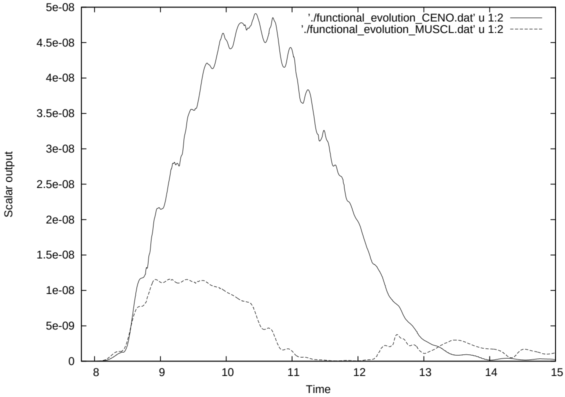

The diffraction of an acoustic wave travelling from a source location to a detector situated in a small region under the "step".

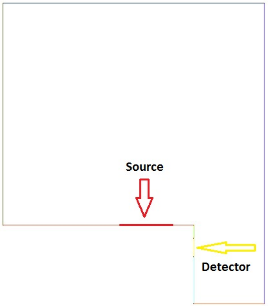

Acoustic source :

$$r = -Ae^{-Bln(2)\left[x^2+y^2\right]}cos(2\pi f).$$

Functional:

$$j(W) = \int_0^T \int_M \frac{1}{2}(p - p_{air})^2 \mathrm{d}M\mathrm{d}t.$$

7. Numerical experiments: Diffraction problem (2)

Density field evolving in time on uniform mesh (line 1), adapted one (middle line), with corresponding adapted meshes (last line):

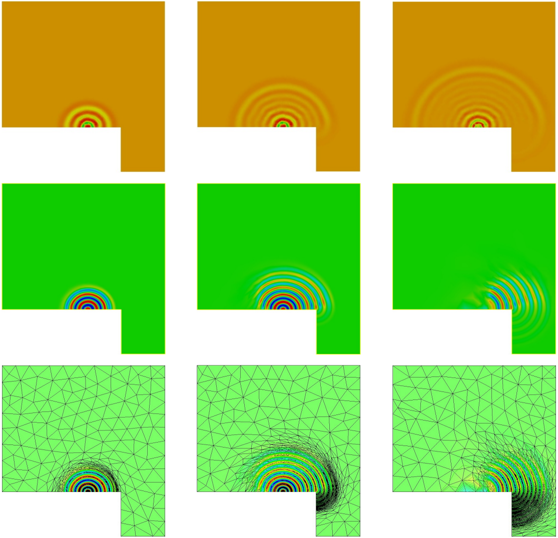

7. Numerical experiments: Diffraction problem (3)

- Our goal-oriented method ensures the accuracy of the functional output $j(W) = \int_0^T \int_M \frac{1}{2}(p - p_{air})^2 \mathrm{d}M\mathrm{d}t$.
- It is thus interesting to analyse the integrand $k(t) = \int_M \frac{1}{2}(p - p_{air})^2 \mathrm{d}M$ of $j(W)$ on the micro M for different sizes of uniform vs. adapted meshes.

7. Numerical experiments: Diffraction problem (4)

Functional time integrand calculation on different sizes of non-adapted meshes (28K, 40K, 68K) vs. adapted meshes (mean sizes: 2620, 4892, 6130).

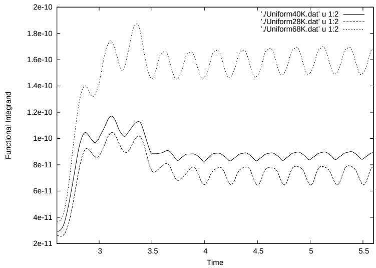

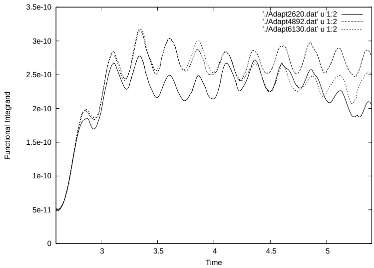

The convergence order is found to be 0.6 for uniform meshes and 1.98 for the adapted one.

7. Numerical experiments: 3rd order error vs 2nd order error

The previous computations where performed with 2nd-order error, made of 2nd-order derivatives, used with the 3rd-order CENO2 scheme.

In a preliminary use of 3rd-order estimate, relying on 3rd-order derivatives, we compare two calculations:
- one with **3rd-order scheme and 2nd-order error**,
- the second with **3rd-order scheme and 3rd-order error**.

The test case is the translation by Euler of a density Gaussian from left to right in a rectangle, with a functional observation with a Gaussian weight at rectangle center.

7. Numerical experiments: Use of 2nd order error

The integrand of the functional is a function of time which culminate when the center of density Gaussian coincides with the center of Gaussian which is the functional weight (center of rectangle).

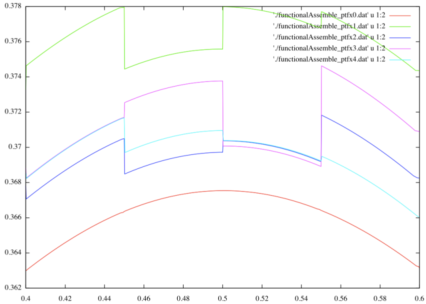

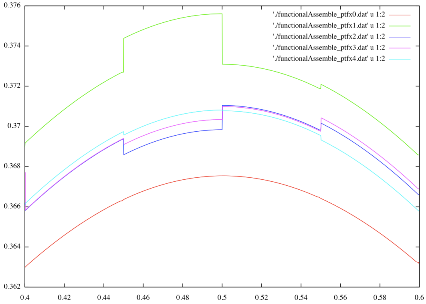

Left, 350 equivalent nodes, right 1500 equivalent nodes.

Here now are the results with the new 3rd-order estimate.

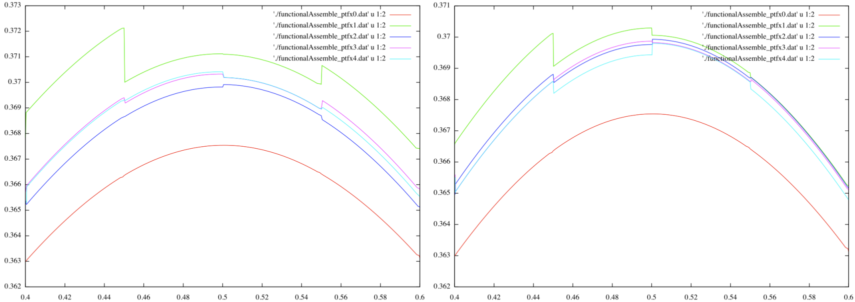

Left, 350 equivalent nodes, right 1500 equivalent nodes.

8. Concluding remarks (1)

A third-order (spatially) accurate goal-oriented mesh adaptation method has been built on the basis of:

• The extension of Hessian analysis to higher order interpolation of Mbinky *et al.*.

• A novel *a priori* analysis.

• The Unsteady Global Fixed-Point mesh adaptation algorithm of Belme *et al.* .

Numerical experiments are yet only 2D and at the very beginning.

8. Concluding remarks (2)

Next studies will address:

- Steady test cases.
- Flows with singularities.
- 3D extension.


MERCI!
THANK YOU!
FRAPAR.